

Distributed Beamforming for Information Transfer in Sensor Networks

G. Barriac
Dept. of Electrical and
Computer Engineering
University of California
Santa Barbara, CA 93106,
USA
barriac@engineering.
ucsb.edu

R. Mudumbai
Dept. of Electrical and
Computer Engineering
University of California
Santa Barbara, CA 93106,
USA
raghu@ece.ucsb.edu

U. Madhow*
Dept. of Electrical and
Computer Engineering
University of California
Santa Barbara, CA 93106,
USA
madhow@ece.ucsb.edu

ABSTRACT

Energy efficient transfer of data from sensors is a fundamental problem in sensor networks. In this paper, we propose a distributed beamforming approach to this problem, with a cluster of sensors emulating a centralized antenna array. While it is well-known that beamforming can provide large performance gains, such gains presuppose not only accurate knowledge of the channel, but also time and phase synchronization at the transmitter. We propose explicit methods for achieving such synchronization in a distributed fashion, and analyze the effects of various sources of coordination error on the attained performance. We find that, as long as the error in range measurements or placement of the sensor nodes is within a fraction of a carrier wavelength, the proposed distributed beamforming strategies achieve most of the gains available from a centralized beamformer.

Categories and Subject Descriptors

H.1.1 [Information Systems]: MODELS AND PRINCIPLES—*Systems and Information Theory*

General Terms

Design

Keywords

sensors, distributed beamforming, synchronization

*This work was supported by the National Science Foundation under grants ANI 0220118 and EIA 0080134, and by the Office of Naval Research under grant N00014-03-1-0090.

Permission to make digital or hard copies of all or part of this work for personal or classroom use is granted without fee provided that copies are not made or distributed for profit or commercial advantage and that copies bear this notice and the full citation on the first page. To copy otherwise, to republish, to post on servers or to redistribute to lists, requires prior specific permission and/or a fee.

IPSN'04, April 26–27, 2004, Berkeley, California, USA.
Copyright 2004 ACM 1-58113-846-6/04/0004 ...\$5.00.

1. INTRODUCTION

In this work, we propose *distributed beamforming* techniques for dramatically increasing the energy efficiency of communication in sensor networks. This technique is complementary to the methods discussed in [3, 6], which address the problem of data relay within a sensor network. In our work, we assume efficient “local communication” (i.e. communication within the sensor field) and show that neighboring sensors are able to coordinate their transmissions to form a distributed antenna array that directs a beam in the desired direction of transmission. The gains from idealized distributed beamforming are known to be large. Our contribution is to provide specific methods for achieving the necessary coordination, and to analyze the effects of various sources of coordination error on the gains obtained.

While there is a cost associated with synchronizing the sensors and for the local exchange of sensor observations, the available SNR (and capacity) gains are compelling. Also one could easily imagine a scenario where individual sensors have a limited transmit power range, so their effective communication distance is constrained by path loss. In this case, the communication distance can be extended considerably by beamforming and the distance can be increased simply by adding more sensors. Figure 8 shows a conceptual view of the sensor field.

In addition to the sensor networks application discussed here, distributed beamforming may also be applicable in more general communication contexts for low carrier frequencies (e.g. 100 MHz or lower), since a standard directional antenna may be difficult to implement at large wavelengths (3 meters or more).

Prior work on distributed beamforming has focused mainly on *receive beamforming*. Perhaps the most dramatic example of this is the Very Large Array (VLA) of antennas used for radio astronomy[4]. Other examples of distributed receive beamforming in the literature include [7, 2]). An example of distributed *transmission* is [8], where the authors propose to use distributed transmit beamforming involving multiple cellular Base Stations to improve the mobile’s SNR. The crucial issues of synchronization required for distributed beamforming are not addressed in this work.

We now provide a brief outline of the rest of this paper. In Section 2, we describe the motivation for, and some requirements for distributed beamforming.

In Section 3, we analyze the effect of the phase noise on receive SNR under a stochastic model for the position error. We also derive simple analytical expressions for the mean and variance of receiver SNR and under Central Limit Theorem assumptions for large N , and obtain an expression for the distribution of SNR as a convolution of two squared Gaussian distributed random variables.

Section 4 describes a simulation model for this system and Section 5 shows results corresponding to the analytical expressions from Section 3. Section 6 concludes the paper with a summary of results and a discussion of possible areas of future work.

2. BACKGROUND

In order to establish the requirements for distributed beamforming, we discuss first the operation of centralized beamforming, i.e., the operation of a standard antenna array. For a transmitter A with n antenna elements, suitably weighting the signals sent from each antenna element can create “beams” in a direction of interest towards receiver B, leading to a factor of n gain in signal-to-noise ratio. Often, such transmit beamforming from A to B could be preceded by training a receive beamformer at A using a transmission from B to A. If the same frequency band is used in both directions, then reciprocity can be used to infer the transmit beamforming weights from the receive beamforming weights. For wideband signaling over certain types of channels, it is even possible to employ different frequency bands in the two directions, and to use *statistical* reciprocity [1] to learn the transmit strategy from A to B, based on what is received at A from B.

However, in order to employ the reciprocity-based method of using weights learnt from receive beamforming, we must be able to perform distributed receive beamforming. To understand the issues involved, consider first the operation of centralized receive beamforming. Assuming that the channel from the transmitter to the receiver is frequency non-selective, the RF signal received at the i th antenna is given by

$$y_i(t) = \text{Re}(s(t)w_i e^{j(2\pi f_1 t + \theta_1)}) \quad (1)$$

where f_1 , θ_1 , are the carrier frequency and phase, respectively, of the arriving wave. Assume that a common carrier frequency and phase of f_0 and θ_0 is employed at each antenna element to demodulate the received signal from RF to baseband. In this case, the complex baseband signal at the i th antenna element is given by

$$s(t)w_i e^{j(2\pi \Delta f t + \gamma)} \quad (2)$$

where $\Delta f = f_1 - f_0$ and $\gamma = \theta_1 - \theta_0$. Assuming that Δf is small enough, the weights w_i can be recovered upto a common phase uncertainty by filtering and sampling the complex baseband signals at a common time. Thus, while it is not required that the receiver lock up to the carrier frequency of the arriving wave, an implicit assumption is the use of a common carrier frequency and phase for demodulation at each antenna element, and timing synchronization of the samples at each antenna element used to estimate the receive beamforming weights. Once the spatial channel $\{w_i\}$ has been estimated, a receive beamformer corresponds to multiplying the complex baseband signal for antenna i by w_i^* . This corresponds to a spatial matched filter. Note that

receive beamformers can also be used to put spatial nulls in the direction of interference, e.g., by computing the beamformer based on a Minimum Mean Squared Error (MMSE) or Minimum Variance Distortionless Response (MVDR) criterion. However, in emulating receive beamforming in a distributed fashion, our first priority is to achieve the simpler task of spatial matched filtering, leaving the issue of distributed interference suppression for later.

Once the receive beamforming weights $\{w_i\}$ have been estimated, if reciprocity applies, they can be used for transmit beamforming. Thus, the complex-valued transmit beamforming weights for a centralized transmit beamformer are given by w_1^*, \dots, w_n^* . If the information to be sent is encoded in the baseband signal $q(t)$, the complex baseband signal transmitted from the i th antenna element is $w_i^* q(t)$. The radio frequency (RF) signal transmitted from the i th antenna is

$$\text{Re}(w_i^* q(t) e^{j2\pi f_0 t + \theta}) \quad (3)$$

where f_0 is the carrier frequency and θ is the carrier phase. The implicit assumptions here are as follows. First, the baseband signals for all antenna elements are synchronized in time. Second, the carrier frequency and phase used to modulate the baseband signals are the same for all antenna elements. These assumptions are easy to satisfy for centralized beamforming, because of the common circuits used to generate the baseband signals and carriers for all antenna elements, and the tight control on the circuit delays in distributing these signals to the antennas.

The preceding discussion reveals that, in order to emulate centralized transmit or receive beamforming in a distributed manner, the key requirements are carrier frequency and phase synchronization, and timing synchronization, among the distributed antenna elements. In the next section, we describe simple methods for achieving such synchronization, and show that the level of precision achieved is sufficient to achieve significant beamforming gains in the direction of interest.

2.1 Methods for Distributed Beamforming

The key concept for achieving the synchronization required for distributed beamforming using a cluster of nodes is to have one node in the cluster serve as a *master* node, broadcasting both a carrier and timing signals. Figure 7 shows the functionality of a sensor node in block diagram form. Assuming that the *slave* nodes in the cluster know their distance relative to the master node, they can lock up to the carrier and timing signals sent by the master, and compensate for the delay with which the master signal arrives, thereby achieving frequency, phase and timing synchronization. The precision with which this synchronization is achieved depends both on the signal-to-noise ratios for the synchronization circuits employed, and on the accuracy of the estimates of the delay between the master and slave nodes. Before discussing implementation of this general concept, we consider a special scenario in which the implementation is particularly simple.

Suppose that the master and slaves are arranged in a star topology, with the master at the center. That is, the master is at approximately equal distance from each slave. This topology could be achieved either by initial placement of the nodes, or, for mobile nodes, by suitable control algorithms that place the slave nodes at a desired distance from the

master. Specifically, slave i is at distance $d(i) = d_0 + d_e(i)$ from the master, where d_0 is the nominal distance, and $d_e(i)$ is the placement error. The required tolerance in placement error is discussed shortly.

The master broadcasts a carrier signal $\cos(2\pi f_0 t)$. Let c denote the speed of light, and $\lambda_0 = \frac{c}{f_0}$ the carrier wavelength. Assuming LOS, slave i receives a noisy carrier signal

$$u_i(t) = \cos(2\pi f_0 t + \theta_0 + \theta_e(i)) + n_i(t)$$

where

$$\theta_0 = \frac{2\pi f_0 d_0}{c} = \frac{2\pi d_0}{\lambda_0}$$

is the nominal phase offset from the transmitted carrier, and

$$\theta_e(i) = \frac{2\pi f_0 d_e(i)}{c} = \frac{2\pi d_e(i)}{\lambda_0}$$

is a phase error resulting from the placement error, and $n_i(t)$ is noise. Each slave employs a phase locked loop (PLL) to lock on to the carrier, whose output can be approximately written as

$$v_i(t) = \cos(2\pi f_0 t + \theta_0 + \theta_e(i) + \theta_{pll}(i))$$

where $\theta_{pll}(i)$ is the phase error due to PLL imperfections and noise. Slave i will employ the carrier $v_i(t)$ for both reception and transmission, as specified in the following.

2.2 Distributed Receive Beamforming

For LOS reception, the received signal at slave i is given by (1). Upon demodulation by the carrier $v_i(t)$, the complex baseband signal at slave i is given by

$$z_i(t) = s(t)w_i e^{j(2\pi\Delta f t + \gamma(i))} \quad (4)$$

where $\Delta f = f_1 - f_0$ and

$$\gamma(i) = \theta_1 - \theta_0 - \theta_e(i) - \theta_{pll}(i)$$

Comparing with (2), we see that the phase variations across different slaves occur due to placement error and PLL error. Thus, if these two errors can be controlled, we can approximate (2) using (4). The PLL error can be made small by increasing the signal-to-noise ratio, which is not difficult if the sensors are relatively close to each other. We therefore neglect it in the following. To understand the requirements on placement error, suppose that we wish to bound $\theta_e(i)$ to within $\delta\theta$, where we might set $\delta\theta = 0.05$ radians, for example. This implies that

$$|d_e(i)| \leq \lambda_0 \frac{\delta\theta}{2\pi}$$

Thus, the smaller the carrier frequency (i.e., the larger the wavelength), the slacker the requirements on placement error for satisfying a desired phase synchronization tolerance. For example, for $f_0 = 10$ MHz and $\delta\theta = 0.05$ radians, we obtain that $|d_e(i)| \leq .24$ meters, which is relatively straightforward to achieve using either manual placement or a suitable control algorithm (in conjunction with a ranging scheme) with mobile sensors. On the other hand, if f_0 is increased to 100 MHz, then the tolerance on the placement error for the same phase tolerance becomes 10-fold more stringent.

Once the required phase tolerance is achieved in the baseband models, it remains to make a measurement of the beamforming gains w_i . One approach for doing this is for the master to broadcast a trigger sequence (possibly in parallel to the carrier it is broadcasting). Suppose, for example,

that the transmitted baseband signal $s(t)$ is a sequence of pulses. Each slave passes the demodulated baseband signal $z_i(t)$ through a pulse matched filter, and makes a measurement of the amplitude and phase at the peak of the matched filter output immediately following detection of the trigger sequence. Note that the trigger sequence arrival time at different slaves is slightly different due to the placement error. Further, the next peak of the matched filter output may occur at slightly different times for different slaves because of the different propagation delays between the transmitter and the slave. However, if the period of the pulses is short enough, and the difference in frequency Δf between the transmitted carrier and the master's carrier is small enough (which is a function of oscillator tolerances), the differences in phase between the measurements at different slaves remains small.

At the end of this process, each slave has an estimate of its own receive beamforming coefficient \hat{w}_i . Distributed receive beamforming can now be performed to enhance the reliability of reception. The details of how this is done depends on the modulation and coding format of the information being received, and we do not discuss this any further here. Instead, we focus attention on how these coefficients would be used for distributed transmit beamforming by exploiting reciprocity.

2.3 Distributed Transmit Beamforming

Once the receive beamforming coefficients have been estimated, transmit beamforming corresponds to implementing a spatial matched filter. The master sends another trigger sequence to initiate transmission from the slaves. It is assumed that the baseband signal $q(t)$ containing the information to be sent has already been agreed upon. Upon receipt of the trigger sequence, slave i modulates the baseband signal $q(t)$ with the carrier at the output of its PLL, sending the RF signal

$$x_i(t) = \text{Re}(\hat{w}_i^* q(t - \tau_e(i)) e^{j(2\pi f_0(t - \tau_e(i)) - \theta_0 - \theta_e(i) - \theta_{pll}(i))}) \quad (5)$$

where $\tau_e(i)$ is the timing synchronization error associated with the receipt of the transmission trigger sequence. The dominant component of this is due to placement error. Letting $\tau_e(i) \approx \frac{d_e(i)}{c}$, and recalling that $\theta_e(i) = \frac{2\pi f_0 d_e(i)}{c}$, (5) can be written as

$$x_i(t) = \text{Re}(\hat{w}_i^* q(t - \tau_e(i)) e^{j(2\pi f_0 t - \theta_0 - 2\theta_e(i) - \theta_{pll}(i))}) \quad (6)$$

If the placement error is small enough to permit accurate distributed receive beamforming, then it is easy to see that it also is small enough for accurate distributed transmit beamforming.

2.4 Beyond the Star Topology

The preceding concepts generalize quite easily beyond the star topology. For a general master-slave topology, it is necessary that each slave has obtained a prior estimate $\hat{\tau}(i)$ of the propagation delay between the master and itself. The required accuracy of this estimate is proportional to the required accuracy in the placement error discussed earlier for the star topology. The master broadcasts a carrier and trigger sequences, and the slaves operate PLLs and detection circuits, as before. However, upon receipt of a trigger sequence, slave i takes a delayed action at time $\tau_0 - \hat{\tau}(i)$,

where τ_0 is an upper bound on the $\{\hat{\tau}(i)\}$. This effectively implements a causal filter which compensates for the variations in delay between the master and different slaves. The analysis of sources of synchronization error are now exactly as in the case of the star topology.

3. ANALYSIS

In this section we determine how placement errors, which translates into phase errors, affect the gains achieved by distributed transmit beamforming. Letting P_R denote the received signal power when the transmit power is kept constant, and letting N denote the number of coordinating sensors, we find that:

(a) The expected value of P_R increases as $\beta_\theta N$, where β_θ is a function of the phase error distribution and $0 \leq \beta_\theta \leq 1$. When there is no phase error, $E[P_R] = N$, meaning that beamforming with N elements gives a power gain of N over transmission with a single element. Thus, the degradation caused by phase errors is contained in the term β_θ .

(b) The variance of P_R also increases linearly with N , for both zero and nonzero phase errors. Of course, the existence of phase errors can only increase the variance over that of an ideal, error free system.

Thus, as long as the distribution of placement errors is contained in such a way as to keep β_θ close to 1, large gains can be still be realized using *distributed* beamforming.

We model the channel coefficients w_i , $i = 1 \dots N$, as circularly symmetric complex normal random variables with zero mean and unit variance, as denoted by $w_i \sim CN(0, 1)$. With the assumption that $\hat{w}_i \approx w_i$, we can write (6) as

$$x_i(t) = \text{Re}(w_i^* q(t - \tau_e(i)) e^{j2\pi f_0 t - \theta_0}) \quad (7)$$

where

$$\hat{w}_i^* = w_i^* e^{-j(2\theta_e(i) + \theta_{pll}(i))} \quad (8)$$

Since the phase locked loop error terms $\theta_{pll}(i)$, $i = 1 \dots N$, can be made arbitrarily small by increasing the signal to noise ratio at the slave nodes when receiving from the master node, we neglect these terms in the subsequent analysis, giving

$$\hat{w}_i^* = w_i^* e^{-j2\theta_e(i)} \quad (9)$$

We also assume that the loss caused by the delays $\tau_e(i)$ in the complex baseband signal is much smaller than the loss caused by the phase errors in \hat{w}_i . This can be justified as follows. Writing $q(t)$ as a pulse train modulated by complex symbols, we have

$$q(t) = \sum_k p(t - kT) s_k \quad (10)$$

where $\{s_k\}$ is the symbol stream, and $p(t)$, $0 < t < T$ is the transmitted pulse. The delays $\tau_e(i)$, $i = 1 \dots N$, in (7) cause both intersymbol interference (ISI) and a reduction in the receive power due to the misalignment of the matched filter. Since the placement errors are (assumed) on the order of $.1\lambda_0$, meaning the timing errors $\tau_e(i)$ are on the order of $\frac{.1\lambda_0}{c}$, and since the pulse duration T is generally on the order of $10\frac{\lambda_0}{c}$ or more, a guard interval on the order of $.01T$ between the transmitted pulses is enough to make ISI negligible. We thus assume that there is such a guard interval and ignore ISI. Also, because the timing error is small compared to the pulse duration T , the resulting loss in the receive signal

strength after matched filtering will be small, on the order of 1%. We therefore concentrate on the loss caused by phase misalignment, since this loss can be on the order of 40% for similar placement errors.

The symbol stream $\{s_k\}$ (see (10)) is normalized so $E[s_k] = 1$, and the power in each pulse, $p(t)$, is normalized to P_T/N , where P_T is the total transmit power, so the power transmitted by all N sensors remains constant at P_T regardless of N . For simplicity of exposition, we set $P_T = 1$. Thus, the baseband representation for the received signal, given that symbol s_k was sent from all N sensors, can be written as

$$r_k = \frac{1}{\sqrt{N}} \mathbf{w}^H \hat{\mathbf{w}}^* s_k + n_k \quad (11)$$

where \mathbf{w} is the $N \times 1$ vector containing the elements $\{w_i\}$, $\hat{\mathbf{w}}$ is defined similarly, and n_k is complex gaussian zero mean noise. Since the index k is arbitrary, we will henceforth drop it from the notation. The received signal power, our figure of merit, is therefore

$$P_R = \frac{1}{N} \|\mathbf{w}^H \hat{\mathbf{w}}^*\|^2 \quad (12)$$

Using (9), this can be written as

$$P_R = \frac{1}{N} \left\| \sum_{i=1}^N \|w_i\|^2 e^{j\theta_f(i)} \right\|^2 \quad (13)$$

where $\theta_f = -2\theta_e$.

Proposition 1: $\frac{1}{N} P_R \rightarrow E[\cos(\theta_f)]$ a.s. as $N \rightarrow \infty$, where a.s. denotes almost sure convergence. In other words, when the total transmit power is kept a constant, the received signal power increases linearly with N as N tends to ∞ .

Proof: We can rewrite (13) as follows:

$$P_R = N \left\| \frac{1}{N} \sum_{i=1}^N \|w_i\|^2 e^{j\theta_f(i)} \right\|^2 \quad (14)$$

Invoking the law of large numbers, and the fact that the $\{\|w_i\|^2\}$, are i.i.d. exponential random variables which are independent from the i.i.d. $\{\theta_f(i)\}$, we have

$$\frac{1}{N} \sum_{i=1}^N \|w_i\|^2 e^{j\theta_f} \rightarrow E[\|w\|^2 (\cos(\theta_f) + j \sin(\theta_f))] \quad a.s. \quad (15)$$

where $w \sim w_i$ and $\theta_f \sim \theta_f(i)$, $\forall i$. The expectation on the RHS of (15) simplifies as follows

$$\begin{aligned} E[\|w\|^2 (\cos(\theta_f) + j \sin(\theta_f))] &= E[\|w\|^2] E[\cos(\theta_f)] \\ &= E[\cos(\theta_f)] \end{aligned} \quad (16)$$

We have assumed that θ_f is symmetrically distributed around 0, and hence $E[\sin(\theta_f)] = 0$. Equation (16) results because $w \sim CN(0, 1)$ and hence $\|w\|^2$ is exponential with unit mean. We thus have that

$$\left\| \frac{1}{N} \sum_{i=1}^N \|w_i\|^2 e^{j\theta_f} \right\|^2 \rightarrow (E[\cos(\theta_f)])^2 a.s. \quad (17)$$

since functions of variables which are converging almost surely also converge almost surely, and the desired result follows. \square

Note that when there are no phase errors, i.e. $f_\theta(\theta') = \delta(0)$, then $\frac{1}{N} P_R \rightarrow 1$ a.s.

Proposition 2: For finite N , $E[P_R] = 1 + (N-1)E[\cos(\theta_f)]^2$. Thus, even for finite N , the expected value of the received signal power increases linearly with N .

Proof: The expected value of P_R can be written as

$$\begin{aligned}
E[P_R] &= \frac{1}{N} E \left[\sum_{i=1}^N \|w_i\|^2 e^{j\theta_f(i)} \sum_{l=1}^N \|w_l\|^2 e^{-j\theta_f(l)} \right] \\
&= \frac{1}{N} \left(N + \frac{N(N-1)}{2} E[\|w_1\|^2 \|w_2\|^2] \right. \\
&\quad \left. 2\Re(e^{j(\theta_f(1)-\theta_f(2))}) \right) \quad (18) \\
&= \frac{1}{N} \left(N + \frac{N(N-1)}{2} 2E[\cos(\theta_f(1) - \theta_f(2))] \right) \\
&= 1 + (N-1)E[\cos(\theta_f(1) - \theta_f(2))] \\
&= 1 + (N-1)E[\cos(\theta_f(1)) \cos(\theta_f(2)) \\
&\quad - \sin(\theta_f(1)) \sin(\theta_f(2))] \\
&= 1 + (N-1)E[\cos(\theta_f)]^2 \quad (19)
\end{aligned}$$

where we have used the fact that the $\{w_i\}, \{\theta_i\}$ are i.i.d. and independent, and that the $\{\theta_i\}$ are symmetrically distributed around 0. \square

In the absence of phase errors, Proposition 2 gives that $E[P_R] = N$.

Proposition 3: When N is large enough for the central limit theorem to apply,

$$P_R \approx X_c^2 + X_s^2 \quad (20)$$

where $X_c \sim N(m_c, \sigma_c^2)$, $X_s \sim N(0, \sigma_s^2)$, and the parameters m_c , σ_c^2 , and σ_s^2 , are given as follows:

$$m_c = \sqrt{N} E[\cos(\theta_f)] \quad (21)$$

$$\sigma_c^2 = 2E[\cos^2(\theta_f)] - E[\cos(\theta_f)]^2 \quad (22)$$

$$\sigma_s^2 = 2E[\sin^2(\theta_f)] \quad (23)$$

The variance of the received signal power is then

$$\text{var}[P_R] = 4\sigma_c^2 m_c^2 + 2\sigma_c^4 + 2\sigma_s^4 \quad (24)$$

which increases linearly with N .

Proof: We once again begin with the definition for P_R .

$$\begin{aligned}
P_R &= \frac{1}{\sqrt{N}} \left\| \sum_{i=1}^N \|w_i\|^2 \cos(\theta_f(i)) + j \sum_{l=1}^N \|w_l\|^2 \sin(\theta_f(l)) \right\|^2 \\
&= \left\| \frac{1}{\sqrt{N}} \sum_{i=1}^N (\|w_i\|^2 \cos(\theta_f(i)) - \alpha) \right. \\
&\quad \left. + j \frac{1}{\sqrt{N}} \sum_{l=1}^N \|w_l\|^2 \sin(\theta_f(l)) + \sqrt{N}\alpha \right\|^2 \quad (25)
\end{aligned}$$

where $\alpha = E[\|w_i\|^2 \cos(\theta_f)] = E[\cos(\theta_f)]$. Invoking the central limit theorem, as N gets large, the first term in (25) tends to a Gaussian random variable with mean 0 and variance $\sigma_c^2 \equiv \text{var}[\|w\|^2 \cos(\theta_f)]$. Similarly, the second term tends to a Gaussian random variable with mean 0 and variance $\sigma_s^2 \equiv \text{var}[\|w\|^2 \sin(\theta_f)]$. Since the last term in (25) is real and constant, it only shifts the mean of the first Gaussian random variable, so we can write

$$P_R \approx \|X_c + jX_s\|^2 \quad (26)$$

where $X_c \sim N(\sqrt{N}\alpha, \sigma_c^2)$, and $X_s \sim N(0, \sigma_s^2)$. Making use of the fact that $\|w\|^2$ is a unit mean exponential random variable,

$$\begin{aligned}
\sigma_c^2 &= \text{var}[\|w\|^2 \cos(\theta_f)] \\
&= E[\|w\|^4 \cos^2(\theta_f)] - E[\|w\|^2 \cos(\theta_f)]^2 \\
&= 2E[\cos^2(\theta_f)] - E[\cos(\theta_f)]^2 \quad (27)
\end{aligned}$$

and similarly

$$\sigma_s^2 = 2E[\sin^2(\theta_f)] \quad (28)$$

Letting $m_c \equiv \sqrt{N}\alpha$, we have that $P_R = X_c^2 + X_s^2$, as given. The variance of P_R follows from standard calculations for moments of Gaussian random variables. \square When there are no phase errors, (24) reduces to $\text{var}[P_R] = 4N$.

4. SIMULATION MODEL

In order to verify the viability of using distributed beamforming, we simulate the sensor system analysed in Section 3 using MATLAB's SIMULINK software. We now describe the simulation methodology and all simplifying assumptions. Figure 6 shows the SIMULINK model of the sensor network.

Because the expected value of the received signal strength, P_R , as given in Proposition 2, remains unchanged when the magnitudes of the $\{w_i\}$ are fixed at 1, and we are interested in finding the empirical value of $E[P_R]$, we can, without loss of generality, let

$$w_i = 1 \quad \forall i \quad (29)$$

We do not model the timing errors $\{\tau_c(i)\}$ in the base band signal (7), since they cause negligible degradation in P_R compared to the phase errors, as mentioned previously. Also, we assume ideal channel estimation, so $\tilde{w}_i = w_i \forall i$. Finally, since we are interested in the receive signal power, and not the received noise power, we do not model the AWGN in (11). Essentially, our simulation modifies (11), and models the following baseband system

$$r_k = \frac{1}{\sqrt{N}} \sum_i e^{j\theta_f(i)} s_k \quad (30)$$

where k is the symbol index and $\{\theta_f(i)\}$ are the phase errors. We assume that the $\{\theta_f(i)\}$ are uniformly distributed around 0, i.e.

$$\theta_f(i) \sim U[-\pi\Delta, \pi\Delta] \quad (31)$$

For each value of Δ and N , we run 60 MonteCarlo simulations to determine $E[P_R]$. Though more averaging is desirable, the time requirements of the simulation make larger numbers of runs impractical.

The sensor data that is transmitted is just a binary pulse train of random bits. The signalling rate is chosen at about 10% of the carrier frequency (i.e. there are about 10 carrier sine wave cycles in a bit interval). The carrier is modulated by multiplying the carrier wave (obtained from the VCO output of the PLL in the sensor's synchronization circuits) with the pulse train. This is equivalent to a BPSK modulated signal, since multiplying the pulse train is the same as a 0 degree phase shift on a "1" bit and a 180 degree phase shift on a "-1" bit.

We assume that the receiver has perfect knowledge of the channel, which is a fairly standard assumption in wireless

receiver design. In this case, this ensures phase synchronization and therefore coherent demodulation is possible. The receiver first converts the signal to baseband by using a mixer to multiply the incoming carrier signal with a local oscillator which is assumed to be frequency synchronized with the transmitting sensors. The mixer is followed by a low-pass filter to remove the unwanted mixer component. Since we are using a rectangular pulse, the baseband matched filtering operation is equivalent to integrating the signal over a bit interval. The square of the integrator output is proportional to the received SNR, and is our figure of merit.

5. RESULTS

In this section, we verify that the SIMULINK simulations match the analytical results, and show how the gains in received signal power scale with N . Using a uniform distribution for the phase errors as given in (31), ($\theta_f(i) \sim U[-\pi\Delta, \pi\Delta] \forall i$), letting $\tilde{\Delta} = \pi\Delta$, and using the approximation $\cos(\theta) = 1 - \frac{\theta^2}{2}$, we have from Proposition 2

$$E[P_R] = 1 + (N - 1) \left(1 - \frac{1}{6} \tilde{\Delta}^2\right)^2 \quad (32)$$

Values of $\frac{E[P_R]}{N}$ computed using (32) are plotted in Figure 1 vs. N along with the values of $\frac{E[P_R]}{N}$ obtained from the MonteCarlo simulations. The top set of lines is for $\Delta = 0.1$, the next set is for $\Delta = 0.2$, and the last two sets are for $\Delta = 0.3$ and $\Delta = 0.4$, respectively. $\Delta = 0.1$ corresponds to a placement error spread of $0.05\lambda_0$, $\Delta = 0.2$ corresponds to a spread of $0.1\lambda_0$, etc. This can be seen by recalling that

$$\theta_f(i) = -2\theta_e(i) \quad (33)$$

and that

$$\theta_e(i) = 2\pi f_o \frac{d_e(i)}{c} \quad (34)$$

where $d_e(i)$ is the placement error. If the $\{d_e(i)\}$ are i.i.d. zero mean uniform random variables over an interval of length $\frac{\Delta}{2} \lambda_0 = \frac{\Delta c}{2f_o}$, then the $\{\theta_e(i)\}$ are uniform over an interval of $2\pi \frac{\Delta}{2}$. In other words,

$$\theta_e(i) \sim U\left[-\frac{\Delta}{2}\pi, \frac{\Delta}{2}\pi\right] \forall i \quad (35)$$

so

$$\theta_f(i) \sim U[-\Delta\pi, \Delta\pi] \forall i \quad (36)$$

and thus $\Delta = 0.1$ corresponds to a placement error spread of $0.05\lambda_0$, etc.

The empirical and analytical results in Figure 1 match well, indicating that the phased locked loop does not introduce any significant errors. We therefore present further results for the analytical model only.

Figure 2 shows how $E[P_R]$ (calculated using (32)) scales with N for discrete values of Δ between 0.1 and 0.4. The maximum slope is 1, corresponding to the case of ideal beamforming. Note that for $\Delta = .4$, at $N = 40$, there is almost a 50% loss compared to this ideal benchmark. However, the expected received signal power is still over 20 times greater than that for a single antenna transmission. Hence, significant gains can still be expected for distributed beamforming.

We now consider how the variance of P_R scales with N . Using the approximations $\cos \theta = 1 - \frac{\theta^2}{2}$ and $\sin \theta = 1 -$

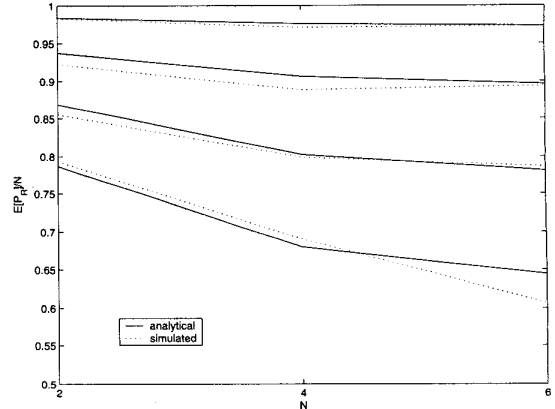


Figure 1: $E[P_R]/N$ vs N , empirical and analytical results. The four sets of curves are for (top to bottom), $\Delta = 0.1 : 0.1 : 0.4$.

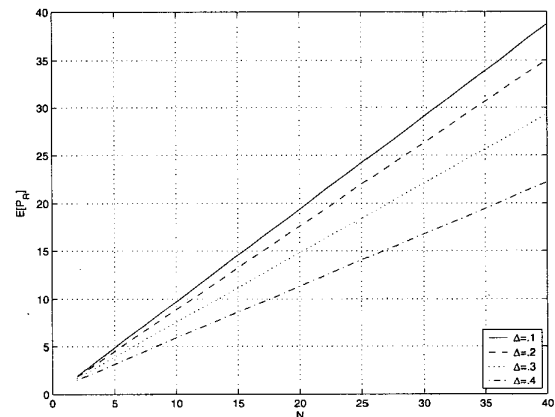


Figure 2: The expected value of the received signal power vs. the number of sensor nodes N .

$\frac{\theta^3}{6}$, as well as the fact that the phase errors are uniformly distributed (36), we can write m_c , σ_c^2 , and σ_s^2 , (defined in Proposition 3), as

$$m_c = \sqrt{N} \left(1 - \frac{\tilde{\Delta}}{6}\right) \quad (37)$$

$$\sigma_c^2 = 1 - \frac{\tilde{\Delta}^2}{3} + \frac{13\tilde{\Delta}^4}{180} \quad (38)$$

$$\sigma_s^2 = \frac{2\tilde{\Delta}^2}{3} - \frac{2\tilde{\Delta}^4}{15} + \frac{\tilde{\Delta}^6}{126} \quad (39)$$

The variance of P_R can then be calculated using (24), and is shown vs. N for various values of Δ in Figure 3.

Histograms of P_R , calculated using the Normal approximations in Proposition 3, are shown in Figure 4 for $\Delta = 0.1$ and $N = 10 : 10 : 40$. Most of the variance is due to variations in $\|w_i\|^2$, as can be seen by comparing Figure 4 to Figure 5, where the magnitudes of the $\{w_i\}$ have been set to

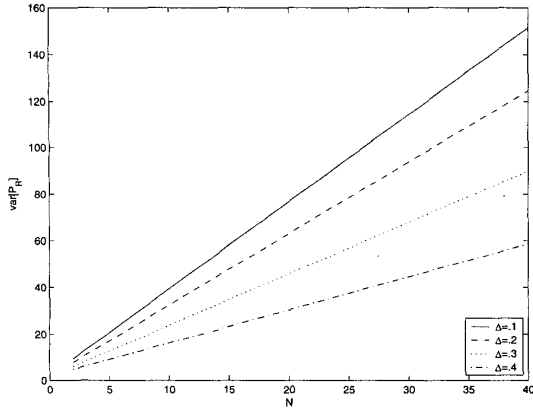


Figure 3: The variance of the received signal power vs. the number of sensor nodes N .

1 \forall . Thus, Figure 5 more accurately captures the variation in received signal power due to synchronization errors.

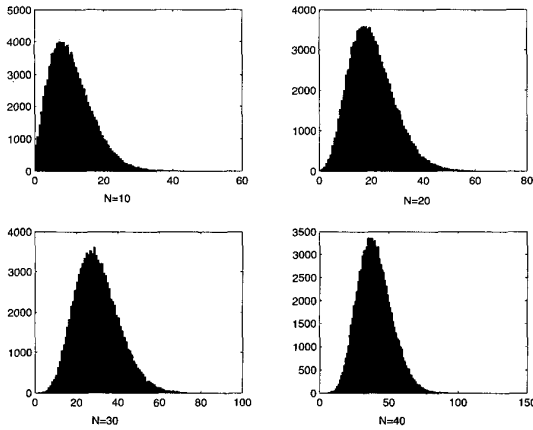


Figure 4: Histograms of P_R . $\Delta = 0.1$

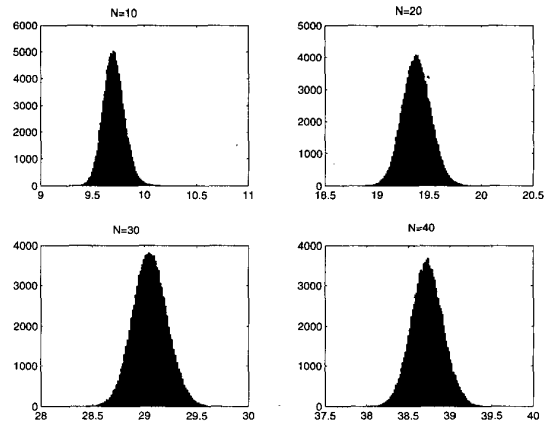


Figure 5: Histograms of P_R where the channel coefficients all have unit magnitude. $\Delta = 0.1$

6. CONCLUSION

We have shown that the large potential gains from distributed beamforming can indeed be realized using a master-slave architecture. Our analysis accurately predicts the performance degradation due to phase noise and range errors.

The crucial assumption in our results is that ranging errors between master and slaves are small compared to the carrier wavelength. An important topic for future work is, therefore to develop architectures for realizing this assumption.

Another important issue is the integration of such techniques with advances in source coding and sensor net organization ([5]) which also point towards a cluster based network architecture.

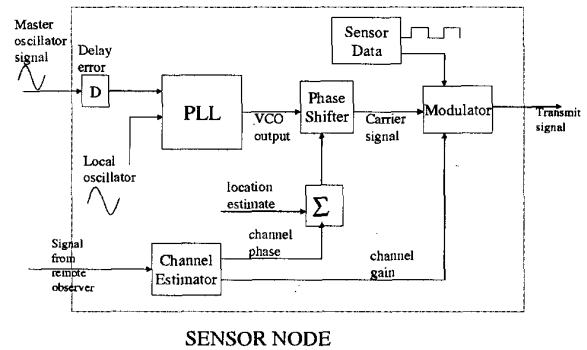


Figure 7: Block diagram of sensor node functionality

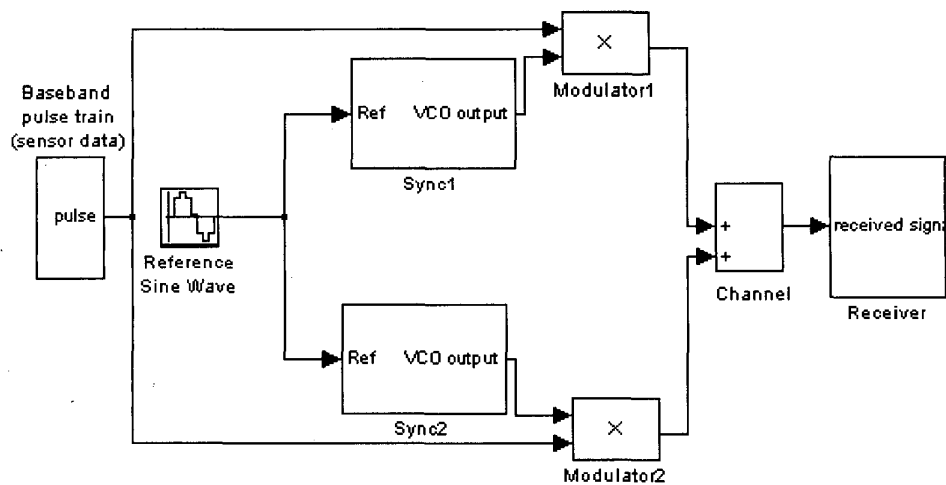


Figure 6: SIMULINK model of beamforming sensors

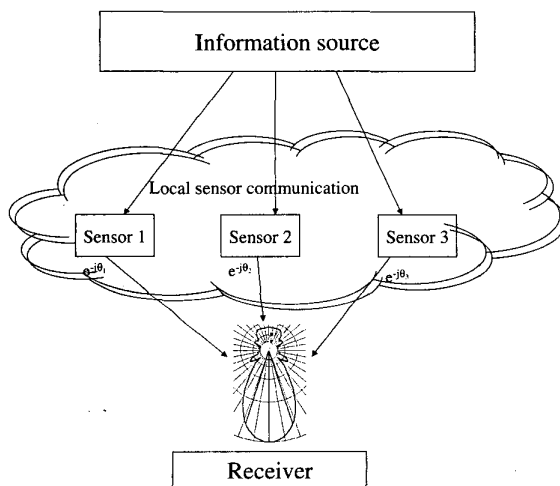


Figure 8: Top level view of sensor field

7. REFERENCES

- [1] G. Barriac and U. Madhow. Space-time communication for OFDM with implicit channel feedback. In *IEEE Global Telecommunications Conference*, volume 3, pages 1321–1325, 2003.
- [2] J. Chen, L. Yip, J. Elson, H. Wang, D. Maniezzo, R. Hudson, K. Yao, and D. Estrin. Coherent acoustic array processing and localization on wireless sensor networks. In *Proceedings of the IEEE*, volume 91, pages 1154 – 1162, August 2003.
- [3] C. Intanagonwivat, R. Govindan, D. Estrin, J. Heidemann, and F. Silva. Directed diffusion for wireless sensor networking. *IEEE/ACM Transactions on Networking*, 11:2–16, February 2003.
- [4] J. D. Kraus. *Antennas, Second Edition*. Mc-Graw Hill, 1988.
- [5] D. Petrovic, R. Shah, K. Ramchandran, and J. Rabaey. Data funneling: routing with aggregation and compression for wireless sensor networks. In *IEEE International Workshop on Sensor Network Protocols and Applications*, pages 156 – 162, May 2003.
- [6] A. Scaglione and S. Servetto. On the interdependence of routing and data compression in multi-hop sensor networks. In *Proc. ACM Mobicom 2002*.
- [7] K. Yao, R. Hudson, C. Reed, D. Chen, T. Tung, and F. Lorenzelli. Array signal processing for a wireless mem sensor network. In *IEEE Workshop on Signal Processing Systems*, pages 11–20, Oct 1998.
- [8] M. Yipeng Tang; Valenti. Coded transmit macrodiversity: block space-time codes over distributed antennas. In *Vehicular Technology Conference*, volume 2, pages 1435–1438, May 2001.